Published in final edited form as:
Adv Funct Mater. 2009 September 23; 19(18): 2969–2977. doi:10.1002/adfm.200900757.

Modulation of Viscoelasticity and HIV Transport as a Function of pH in a Reversibly Crosslinked Hydrogel**

Julie I. Jay
Department of Pharmaceutics and Pharmaceutical Chemistry University of Utah, Salt Lake City, UT 84112-5820 (USA)

Shetha Shukair
Department of Cell and Molecular Biology, Feinberg School of Medicine, Northwestern University Chicago IL, 60611 (USA)

Kristofer Langheinrich
Department of Bioengineering, University of Utah Salt Lake City, UT 84112-5820 (USA)

Melissa C. Hanson
Department of Bioengineering, University of Utah Salt Lake City, UT 84112-5820 (USA)

Gianguido C. Cianci [Dr.]
Department of Cell and Molecular Biology, Feinberg School of Medicine, Northwestern University Chicago IL, 60611 (USA)

Todd J. Johnson
Department of Bioengineering, University of Utah Salt Lake City, UT 84112-5820 (USA)

Meredith R. Clark [Dr.]
Department of Bioengineering, University of Utah Salt Lake City, UT 84112-5820 (USA)

Thomas J. Hope [Prof.]
Department of Cell and Molecular Biology, Feinberg School of Medicine, Northwestern University Chicago IL, 60611 (USA)

Patrick F. Kiser* **[Prof.]**
Department of Pharmaceutics and Pharmaceutical Chemistry University of Utah, Salt Lake City, UT 84112-5820 (USA)

Department of Bioengineering, University of Utah Salt Lake City, UT 84112-5820 (USA)

Keywords

pH responsive material; viscoelastic properties; inhibition HIV transport; phenylboronic acid; microbicide

**We thank Chris Rodesch, Ph.D and Keith Carney of the University of Utah Fluorescent Microscopy Core Facility for their assistance in setting up the microscopy analysis for the particle tracking experiments. We are also grateful to Eric R. Weeks, Ph.D, Associate Professor in the Department of Physics at Emory University, for his assistance and for providing the IDL code for particle tracking and MSD analysis. This work was supported by the NIH, grant number R21-AI062445 (P.K.), T32-AI060523 (S.S), and R33-AI076968 (T.J.H).

*patrick.kiser@utah.edu.

pH modulates the viscoelasticity and HIV transport in hydrogels created by the pH sensitive equilibrium between polymer bound phenylboronic acid (PBA, blue) and salicylhydroxamic acid (SHA, green). At vaginal pH the PBA-SHA crosslink rapidly hydrolyzes and reforms yielding viscoelastic gels. Above pH 5.5 the rate of hydrolysis decreases resulting in more permanently covalent crosslinks and elastic gel behavior that impedes HIV transport.

Materials that respond to physiological stimuli are important in developing advanced biomaterials for modern therapies. The reversibility of covalent-crosslinks formed by phenylboronate (PBA) and salicylhydroxamate (SHA) has been exploited to provide a pH-responsive gel for application to the vaginal tract. Dynamic rheology reveals that the gel frequency-dependent viscoelastic properties are modulated by pH. At pH 4.8 the viscous component dominates throughout most of the frequency range. As the pH increases, the characteristic relaxation time continues to increase while the $G'_{Plateau}$ levels off above pH 6. At pH 7.5, the elastic component dominates throughout the frequency sweep and is predominately independent of frequency. Particle tracking assessed the transport of both fluorescently labeled HIV-1 and 100 nm latex particles in the PBA-SHA crosslinked gel as a function of pH. At pH 4.8 the ensemble-averaged mean squared displacement at lag times greater than three seconds reveals that transport of the HIV-1 and 100 nm particles becomes significantly impeded by the matrix, exhibiting diffusion coefficients less than 0.0002 $\mu m^2 s^{-1}$. This pH responsive gel thus displays properties that have the potential to significantly reduce the transport of HIV-1 to susceptible tissues and thus prevent the first stage of male-to-female transmission of HIV-1.

1. Introduction

New functional materials capable of modulating their properties based on biological cues are a continued focus of study in advanced drug delivery vehicle design.[1] One primary focus in this area is novel polymeric systems that provide mechanisms for triggered physiological modulation of material properties.[2–4] We apply these principles to develop new materials to improve the performance of microbicides. Microbicides are topical drug delivery systems containing anti-HIV-1 active agents for vaginal delivery to locally prevent the sexual transmission of HIV-1.[5] Of particular interest are new materials that sense the presence of HIV-1 or HIV-1 containing fluids and rapidly modulate their transport properties in response to this stimulus to create a barrier that inhibits interaction of HIV-1 with susceptible tissues and cells.

Rational design of new polymeric systems to create improved microbicide vehicles inevitably derives from knowledge of vaginal physiology and the initial factors involved in male-to-female HIV-1 transmission. The precoital pH of the vaginal fluid is normally acidic, ranging from 4 to 5 except in the presence of semen where the lumen environment is neutralized due to semen's slightly alkaline pH, higher buffering capacity and larger volume.[6, 7] HIV-1 transmission begins with advective or diffusive transport of virions from infected seminal fluid to the vaginal mucosal surface; a process which occurs over a timescale of minutes.[8, 9] The virions have been shown to then penetrate through the mucosal barrier and the epithelium where they come into contact with susceptible immune cells in sub-epithelial tissue.[8, 10, 11] Based on the evidence that viral penetration of cervicovaginal mucosa to the intra-epithelial space is an initial step in infection,[12] the use of a microbicide gel that prevents transport of virus to vulnerable tissue would constitute an important mechanism in preventing the heterosexual transmission of HIV-1. Modeling of viral transport and in vitro experiments of placebo microbicide gels has suggested that layers as thin as 100 μm could significantly delay viral transport to tissue, providing time for the innate vaginal defenses and local antiviral agents to inactivate the virus.[13, 14]

The challenge in engineering a gel that acts as a barrier in this context is that the viscosity that promotes the topical distribution of the gel[15] generally may not contain a sufficient crosslink density to prevent virion penetration through the gel layer. A pH responsive gel provides an opportunity for tuning viscoelastic properties to attain a low viscosity gel at acidic vaginal pH for application and a more elastic gel at neutral pH to prevent transport of virus.

We describe for the first time the transport properties of HIV in a hydrogel material based on the pH-sensitive reversible covalent bonds formed between phenylboronic acid (PBA) and the diol-containing salicylhydroxamic acid (SHA) moiety.[16–19] Boronic acid undergoes a well-known condensation reaction with 1,2- or 1,3-diols to form five or six membered cyclic esters. This condensation reaction is reversible and highly influenced by the pH and chemical structure of the diols.[20] Conversion of the boronic acid to the charged boronate tetrahedral conformation yields a more stable complex that resists hydrolysis compared to its trigonal form of the complex which is more readily reversible. This complex formation and dissociation of cyclic boronic acid esters with diols has been harnessed by others in drug delivery system engineering.[21–23]

We selected the complex formed from PBA with SHA due to the shifting pH range of 4–7 that occurs in the vaginal lumen.[16, 17] The PBA-SHA complex is unique in its ability to exist in the tetrahedral boronate conformation even at slightly acidic pH values[18, 19] compared to other diol complexes in which PBA predominantly exists in its tetrahedral configuration only at alkaline pH.[20] The behavior of the reversible pH-sensitive PBA-SHA crosslink therefore has the potential to provide bioresponsive modulation of the gel's viscoelastic properties. At acidic pH where significant hydrolysis of the trigonal PBA-SHA complex occurs, few crosslinks will exist, resulting in a low viscosity gel. Upon neutralization the PBA-SHA complex will exist predominantly in the tetrahedral conformation forming stable complexes and a densely crosslinked matrix that could act as a physical barrier to HIV-1 transport (Scheme 1).

In this paper we characterize the pH sensitivity of the PBA-SHA crosslink equilibrium in terms of how crosslink lifetime, and thus the extent of crosslinking, impacts dynamic gel rheological properties and the Brownian motion of HIV-1 and nanoparticle diffusion in the gel acidic pH while the elastic behavior dominates with increasing pH. The Brownian motion of HIV-1 and nanoparticles decreases as a function of pH with movement slowing by almost three orders of magnitude from pH 4.3 to pH 4.8.

2. Results and Discussion

2.1. Gel composition

We have previously explored the chemorheological properties for poly(hydroxypropylacrylamide) (pHPMAm) based PBA-SHA crosslinked hydrogels as a function of substitution and concentration at pH 4.2, 5.5 and 7.6.[16, 24] P(HPMAm) was chosen as the polymer backbone based on its high water solubility and biocompatiblity.[25] Our previous results were assessed to identify a composition that demonstrated dynamic reversible behavior and a dynamic gel strength ($G'_{Plateau}$) between 10 and 50 Pa in the vaginal pH range of 4 to 5. Gels in this range have viscosities similar to current microbicide gel formulations with viscosities of 5 to 50 Pa s (unpublished data). Due to the more dynamic gels formed with the 5 mol% polymers compared to higher degrees of substitution,[16] this degree of functionalization was chosen for further characterization as a microbicide gel. The final polymer concentration, 75 mg mL^{-1}, was chosen to obtain a $G'_{Plateau}$ within the desired range of 10 to 50 Pa at vaginal pH. Five mole percent polymers were synthesized by free radical polymerization (Figure 1). For p($HPMAm_{95}$-$APMAmPBA_5$) (1) the average mole percent of PBA was 4.4% and in p($HPMAm_{95}$-$MAAmSHA_5$) (2) the average mole percent of SHA was 5.95% as determined by ^1H NMR in D_2O. Absolute M_w and M was determined using GPC equipped with a differential refractive index detector and a multi-light scattering detector. The average M_w and M_n for all polymers used here are 171/138 KDa (1) and 236/142 KDa, (2). The gel was formulated in a 100 mM pH 4.8 acetate buffer. For characterization of the viscoelastic properties of the

gel at other pH's, the polymers were formulated at 75 mg mL^{-1} in the appropriate 100 mM buffer.

2.2. Rheological characterization

The frequency dependence of the PBA-SHA crosslinked gel's viscoelastic properties was investigated over the pH range of 4 to 8 to assess how pH affects the viscoelastic behavior of the gel structure (**Figure**). This pH range covers the normal vaginal pH to the slightly alkaline pH experienced by the vaginal lumen in the presence of seminal fluid.[7] The PBA-SHA crosslinked hydrogel displays rheological behavior that is consistent with time-dependent dynamic gel networks with transient crosslinks.[26] This is due to the equilibrium of the pH responsive PBA-SHA complex.[24] The formation of the more stable tetrahedral PBA-SHA complex is pH dependent, occurring in greater proportion with increasing pH. At more acidic pHs this complex is in equilibrium with the more rapidly hydrolyzed trigonal PBA-SHA complex and the rate of dissociation of these crosslinks impacts the viscoelasticity of the gel. The crosslink lifetime is therefore highly dependent on the boronic acid-diol equilibrium and thus on pH.[19, 24] The ensemble lifetime of the gel crosslinks is characterized by the gel relaxation time, τ. It can be measured by evaluating the frequency dependence of the viscous and elastic moduli and is defined as the inverse of the crossover frequency (in Hertz) where G' equals G".[17, 27] For gels utilizing a boronic acid-diol complex as the crosslink, τ is indicative of the crosslink lifetime that then impacts the extent of crosslinking at any given moment.[16, 17, 27–29]

At pH 4.8 the crossover frequency in Hz corresponds to a relaxation time of 0.9 s (**Figurea**). At this slightly acidic pH the PBA-SHA crosslink is likely to be predominately in the trigonal form and thus highly labile due to rapid hydrolysis. This results in the gel demonstrating predominately viscous-dominant behavior throughout most of the frequency sweep. The rapid restructuring due to dissociation of the PBA-SHA crosslink thus yields a gel with the capacity for flow and may therefore have the appropriate properties to coat tissue induced by squeezing flows.[30, 31] As the pH increases, τ continues to increase to longer and longer time scales. At pH 5.5 the characteristic relaxation time is 10.5 s and at pH 7.5 it has increased to 160 s. As the pH increases PBA converts to its tetrahedral conformation which stabilizes the PBA-SHA complex against hydrolysis and results in the gel exhibiting longer τ. This corresponds to an increasing dominance in the elastic modulus, G', over the majority of the frequency sweep as the pH rises. At pH 7.5 G' is virtually independent of frequency over the range tested indicating the formation of a covalently crosslinked gel network.[32]

The pH dependent behavior of the PBA-SHA crosslink also impacts the overall dynamic gel strength, measured by the elastic plateau modulus, $G'_{Plateau}$, which is determined from the average G' over the plateau region of the frequency sweep (**Figureb**). A rapid increase in the $G'_{Plateau}$ occurred in the vaginal pH range of 4.8 to 5.5 increasing from an average of 11 Pa to 380 Pa across this pH range. Above pH 6 the $G'_{Plateau}$ leveled off around 1,000 Pa, however, over this pH range, τ continues to increase. We hypothesize that under these conditions it is possible that the gel network has reached a sterically constrained maximal crosslink density that is not significantly impacted by the increased relaxation time of the crosslink.[24] The leveling off of the elastic plateau modulus may also indicate the polymers have obtained a minimum network mesh size that can not be made smaller due to steric limitations in chain mobility in the crosslinked backbones. These results indicate that the PBA-SHA crosslink, and gels of the above composition, provide a system with tunable viscoelasticity. The PBA-SHA gel can be applied as a low viscosity gel formulated for the slightly acidic vaginal environment. Exposure to seminal plasma and neutralization of the vaginal lumen will induce an increase in crosslink density and likely minimize mesh size.

2.3. HIV-1 and nanoparticle transport

A change in the density and ensemble lifetime of the crosslinks could impact transport of the 110 to 128 nm mature HIV-1 virions[33] through the network. The effect pH, and thus the viscoelastic properties of the gel, have on transport was assessed by tracking single Gag-Cherry labeled HIV-1 (BaL strain) virions[34] in the gel at different pHs. Video particle tracking was used to characterize trajectories of virions in the gels[35] and to calculate the individual mean squared displacement (MSD, $<\Delta r^2(t)>$, Figure 4) and the ensemble-averaged mean squared displacements of the virions at each sample condition. Analysis of the individual HIV-1 virions provides insight into how the microenvironment of the PBA-SHA network impacts transport of each virion. The spread of the individual MSD reflects the uncertainties due to statistical fluctuations that result from short data collection times imposed by photobleaching and possibly the heterogeneity of the sample.[36] The individual MSDs are plotted out to one second because statistical accuracy is best at short lag times.

At pH 4.3 where the polymer mixture is a viscous liquid, the virions diffuse the most rapidly. At pH 4.5 a reduction in the individual MSD slopes for the majority of the virions occurs, demonstrating that their motion within the gel network is becoming increasingly constrained. It is possible that a sufficient number of transient crosslinks increase the local viscosity around the virions thus inhibiting their movement. Viral displacement then becomes significantly impeded at and above pH 4.8. The individual virion MSDs show limited displacement even at the shortest lag time, and apparent plateaus for lag times greater than 0.1 s out to 1 s. Correspondingly, as the pH increases, the shortened trajectories of virions indicate that they are entrapped in continuously shrinking pockets likely due to decreasing mesh size of the gel network and/or increasing viscosity in the local microenvironment. Both scenarios would occur due to formation of increasingly stable PBA-SHA crosslinks (**Figure**).

We are interested in comparing the transport of HIV-1 to particles with a known size and homogeneous surface chemistry, and thus characterized the mean-squared displacement of 100 nm sulfate modified latex particles in the gel network as a function of pH. Sulfate modified particles were chosen in order to provide a completely negative surface at all pH's tested that should minimize colloidal interactions with the polymer backbones.

The individual MSDs of 100 nm beads reveal the same general trend as the HIV-1 virions, a continued overall decrease in the slope of the MSD versus t with increasing pH (MSD, $<\Delta r^2(t)>$, **Figure**). However unlike the virions at pH 4.5, the 100 nm beads do not display as significant a reduction in the slopes of the individual MSDs. Rather the majority of particles display an increase in their MSD values over HIV-1 with increasing lag times up to one second, though the slopes appear to be lower than the beads in the gel at pH 4.3. This suggests that the 100 nm sulfate beads are not as constrained by the gel network as HIV-1 at this pH and that a mechanism other than size, likely associated with differences in surface chemistry, may be impacting transport of the virions in gels at pH 4.5. At pH 4.8 and 5.5, the 100 nm beads, like the virions, exhibit apparent plateaus occurring above a lag time of 0.1 s suggesting that the particles do not move above our detection threshold likely due to physical entrapment caused by minimization in the mesh size below 100 nm.

The ensemble-averaged MSDs of HIV-1 and 100 nm beads (MSD, $<\Delta r^2(t)>$, **Figure**) were also compared to provide information about the behavior of each type of particle with greater statistical accuracy and also to allow us to analyze the MSD at longer lag times.[36] At pH 4.3 HIV-1 and 100 nm beads display identical diffusive behavior. At pH 4.5 the 100 nm beads and HIV-1 display subdiffusive behavior with power-law slopes below one at very short lag times, with the virions remaining impeded approximately three times longer than the nanoparticles. This suggests that a mechanism other than size may be hindering virion

transport through the gel matrix at pH 4.5. As the pH increases HIV-1 and the 100 nm beads display almost identical behavior suggesting that size alone appears to dominate transport phenomenon in the gel at higher pHs. For the 100 nm beads, the plateau exhibited at pH 4.8 and pH 5.5 is just above the experimental noise level. For HIV-1 the plateaus are below the noise level limiting conclusive ability to determine subdiffusive behavior and caging effects the matrix may have on the particles. The upward slope at pH 4.8 at lag times greater than three seconds, where power law behavior with a slope of one is obeyed, does approximately correlate with the time scales in the dynamic frequency sweeps where the viscous component dominates. We also analyzed 50 nm sulfate modified beads at each pH. At all pHs tested, the differences in the ensemble-averaged MSD of the 50 nm and 100 nm were indistinguishable due to experimental noise levels (data not shown).

The ensemble-averaged MSD at lag times where the power law behavior exhibits a slope of one, as depicted by the solid line in Figure 7, were used to determine the diffusion coefficients of HIV-1 and the 100 nm beads (Figure 8). These values were then used in the Stokes-Einstein equation to determine the viscosity of the PBA-SHA gel at each pH. At pH 4.3 the diffusion coefficient for HIV-1 and the 100 nm beads was 6×10^{-2} μm^2 s^{-1} (6×10^{-10} cm^2 s^{-1}) corresponding to a viscosity of 0.073 Pa s. At pH 4.5 HIV-1 displays a lower diffusion coefficient than the 100 nm polystyrene beads, corresponding to a higher viscosity of 6.2 Pa s compared to 1.3 Pa s, respectively. The greater viscosity exhibited by the virions may be explained by surface interactions with the polymer matrix resulting in slower transport than the 100 nm beads. At pH 4.8 HIV-1 and the 100 nm have similar diffusion coefficients corresponding to viscosities of 33 Pa s and 58 Pa s, respectively. The simple viscosity tested by macrorheology yielded an average viscosity of 25 Pa s (data not shown). Overall, the almost three fold order of magnitude drop in the diffusion coefficient of HIV-1 and the 100 nm beads over a pH range of 4.3 to pH 4.8 demonstrates the dramatic ability of the PBA-SHA crosslinked gel to respond to pH and diminish viral transport.

While HIV-1 in general follows a similar trend in decreasing MSD values and diffusion coefficients as the 100 nm sulfate nanoparticles, the individual MSD and ensemble-averaged

MSD for virions behavior differs at pH 4.5 from the 100 nm beads. At this pH the decrease in transport of the virions compared to the negatively charged sulfate particles may occur due to chemical interaction of the HIV-1 surface proteins with the functionalized polymers. Bonding interactions between the polymer backbone or free crosslinking moieties and the viral envelope may slow the movement of some of the viral population. Surface chemistry and chemical interaction with the surrounding matrix is known to influence transport of virions and other functionalized particles through mucus,[37–39] the extracellular matrix[40] and hydrogels.[41] The decreased diffusion of the HIV-1 population at pH 4.5 could be due to phenylboronic acid's ability at acidic pH to bind to terminal sialic acid residues found on glycosylated regions of the HIV-1 envelope fusion protein gp120.[42, 43] These interactions may account for some of the variability between viral diffusion compared to the similar sized 100nm sulfate nanoparticles at pH 4.5.

At and above pH 4.8, physical entrapment is likely the predominant means for inhibition of transport due to minimization of the network mesh around the HIV-1 and 100 nm beads. The PBA-SHA crosslinked gel therefore demonstrates the ability to diminish viral transport at pH 4.8 even though the gel displays a transient network with a characteristic relaxation time of less than one second. Even when diffusive behavior occurs at lag times greater than three seconds, HIV-1 displacement was greatly limited. This result is likely impacted by the mesh size of the polymer network, which may yield mesh sizes less than 100 nm in between the transient crosslinks. Above pH 5.5 where G'Plateau levels off and the gel's characteristic

relaxation time increases to timescales on the order of minutes the polymer mixture will likely decrease transport even further at pHs closer to seminal plasma.

Based on the ensemble-averaged MSD, HIV-1 in the pH 4.8 PBA-SHA crosslinked polymers would move by Brownian motion an average of 3.4 μm in six hours, approximately the time required for the vaginal environment to reacidify.[7] Above pH 4.8 the characteristic relaxation time and dynamic gel strength rapidly increase suggesting that exposure to seminal fluid will create a layer capable of decreasing HIV-1 transport even further. As the vaginal environment reacidifies after neutralization from semen, a 100 μm layer of a vaginally applied PBA-SHA gel could provide a matrix capable of halting viral transport, while providing time for the innate vaginal defenses and locally delivered pharmacological agents to inactivate the virus. The PBA-SHA crosslinked gel is thus capable of preventing transport likely through physical entrapment and possibly chemical interactions with surface proteins on the HIV-1 envelope providing a material with the facility to attenuate HIV-1 infection by preventing the first step in the HIV-1 lifecycle.

3. Conclusions

Due to the recent Phase III clinical trial failures of microbicides containing anionic polymers as the active pharmaceutical ingredient, the international research community is reevaluating its focus on next generation microbicides.[44] One aim in the development of next generation microbicides is to prevent HIV-1 infection at multiple steps in the infection lifecycle. For the first time we demonstrate the possibility of engineering a vehicle to participate in the prevention of the first step in the sexual transmission of HIV-1. Since the first step in heterosexual transmission is advective and diffusive transport of virions from seminal fluid to the cervicovaginal mucosa, we designed a gel with the capacity to respond to the increase in pH induced by seminal plasma at the onslaught of viral exposure by becoming a densely crosslinked hydrogel impermeable to viral transport. The use of the PBA-SHA crosslink also addresses issues in regards to tissue biodistribution by providing a gel capable of viscous flow at acidic pH. We therefore believe the development of pH-responsive microbicide vehicles based on the reversible covalent nature of the PBA-SHA crosslink has the potential to act as a barrier to HIV-1 penetration and diffusion, and therefore to significantly reduce the available titre of the infectious agent. The progression of the use of intelligently designed vehicles for drug delivery in the microbicide field thus has the opportunity to provide women with an improved means to protecting themselves from the heterosexual transmission of HIV-1.

4. Experimental

Materials

The following materials were purchased from Sigma-Aldrich, Inc., St. Louis, MO: Methacryloyl chloride, sulfate modified polystyrene beads, and 2,2'-azobisisobutyronitrile (AIBN). AIBN was then recrystallized from chloroform in a chloroform-N_2(l) bath. Dubelco's modified eagles media (DMEM High Glucose) was purchased from HyClone Laboratories, Logan, UT. All other chemicals and reagents were purchased from Aldrich or Acros and used without further purification unless otherwise noted. Dimethylformamide (DMF) and ethyl acetate were dried over 4 $\mathring{A}$ molecular sieves. Thin layer chromatography plates were purchased from Whatman (aluminum backing, UV fluorescence 254 nm, silica gel, Kent, UK). All ^{1}H NMR spectra were acquired on a Varian Mercury 400 MHz spectrometer. ^{1}H chemical shifts arec reported as δ referenced to solvent and coupling constants (*J*) are reported in Hz. Polymer molecular mass distributions were determined in deionized distilled (DDI) water or HPLC grade DMF using gel permeation chromatography

(GPC) (HPLC 1100, Agilent Technologies) equipped with an aqueous column (PLaquagel-OH mixed, Polymer Labs) or an organic column (PLgel mixed-B, Polymer Labs), a differential refractive index detector (BI-DNDC, Brookhaven Instruments) and a multi-angle light scattering detector (BI-MwA, Brookhaven Instruments). DDI water was used in all experiments. A polymer standard (polyethyleneoxide (PEO), Varian Inc) was prepared at 1 mg mL^{-1} in DMF and used to calibrate the instrument. For buffered samples the pH was adjusted with an Accumet microprobe (Cole-Parmer) after 3 point calibration at pH 4, 7 and 10.

Functionalized Monomer synthesis

The synthesis of the phenylboronic vinyl monomer, N-[3-(2-Methyl-acryloylamino)-propyl]-4-amidophenylboronic acid (APMAmPBA), and the SHA vinyl monomer, 4-[(2-Methyl-acryloylamino)-methyl]-salicylhydroxamic acid (MAAmSHA) were synthesized according the previously published protocols [17].

2-hydroxypropylmethacrylamide (HPMAm)

1-amino-2-propanol (73.8 mL, 957 mmol) was added to a 1 L straight three neck round bottom flask followed by 500 mL ethylacetate, 4Å. The flask was equipped with an overhead stirrer (Caframo RZR 2000, Digital 2000), thermometer and a 100 mL constant addition funnel. To the addition funnel was added a freshly opened bottle of methacryloyl chloride (97%) (Fluka, 48 mL, 478 mmol). Ethyl acetate, 4Å, (70 mL) was added to the addition funnel to dilute the methacryloyl chloride, and stirred to create a homogenous solution. The reaction chamber was flushed with N_2 (g) while the bulk reaction was cooled to −20°C in an ethanol-dry ice bath. The methacryloyl chloride solution was added drop wise at a rate of 1 drop/sec. After addition, the reaction was warmed to room temperature and stirred for an additional 3 hours. TLC showed reaction had gone to completion (R_f = 0.3 HPMAm, R_f = 0.1-amino-2-propanol hydrochloride in 90:10 chloroform:methanol). Upon completion of reaction, the white solid (1-amino-2-propanol hydrochloride) was filtered off and rinsed with ethyl acetate (100 mL). The combined reaction supernatant and rinse were placed in a −20°C freezer. After 24 hours, white crystals of product had formed. Crystals were collected via vacuum filtration and rinsed with chilled ethyl acetate and dried under high vacuum. The remaining white solid from the filtered mother liquor still showed HPMAm by TLC. The solid was rinsed with acetone (3 times 100 mL) and concentrated. This was then redissolved in ethyl acetate (500 mL) and recrystallized for 24 hours at −20°C. Crystals of HPMAm were filtered and dried over hi-vac for a combined yield of 44 g, 307 mmol, 65% yield) and characterized by ^1H NMR (400 MHz, $CDCl_3$) δ 6.51 (br, 1H), 5.689 (s, 1H), 5.303 (s, 1H), 3.904 (m, 1H), 3.452 (m, 1H), 3.126 (m, 1H), 1.920 (s, 3H), 1.146 (d, 3H, J=6.25).

Polymer synthesis

Several batches of functionalized polymers were synthesized by free radical polymerization as previously described (Figure 1) [17]. Polymers were synthesized with a mole ratio of 95:5 by free radical polymerization using HPMAm with either APMAmPBA or MAAmSHA monomers. Polymerizations were performed using 25% w w^{-1} monomers with AIBN (0.6 mol% of the total monomer feed) in dry DMF (75% w w^{-1}) at 65°C for 24 h under nitrogen atmosphere. Polymers were triturated in acetone, redissolved in methanol and triturated two more times in acetone. After the first trituration PBA-containing polymers were deprotected by acidifying the methanol with a 1:1 dilution of 1 M HCl for 30 min at room temperature. Polymers were then lyophilized. Polymers were ultracentrifuged four times prior to any viral transport assay using Amicon Ultra-15 10K MWCO dialysis centrifuge tubes (Millipore) at a polymer concentration of 25 mg mL^{-1}. The first pass filtration was performed using 100 mM pH 7.5 PBS buffer and the next three purification passes used DDI water. Samples were

centrifuged at 3,000 rpm for 90 min. Actual molar feed ratios of polymers were determined in ^{1}H NMR in D_2O. For **1** the average mole percent of PBA was 4.4% and in **2** the average mole percent of SHA was 5.95%. M_w M_n^{-1} was determined in HPLC grade DMF or DDI water by GPC. The average M_w and M_n for all polymers used here are 171/138 KDa and 236/142 KDa respectively.

Dynamic Rheology

Polymers **1** and **2** were individually dissolved in buffer (100 mM acetate, MES, citrate or phosphate buffer) at 75 mg mL^{-1} concentrations. Any pH adjustments were performed with either 1 M HCl or 1 M NaOH before diluting to the final concentration. Gels were formed in situ by simultaneously pipetting an equal volume of **1** and **2** in solution directly onto the rheometer's Peltier plate.

Dynamic rheology was performed using methods similar to those previously described using a cone-and-plate configuration on a stress-controlled rheometer (AR550, TA Instruments) [17]. Briefly, a steel, 4° cone-shaped, 20mm diameter geometry was used for all experiments with a total sample volume of 170 μL. Time sweeps were performed at 25°C at a small amplitude oscillatory stress (1–10 Pa) and small angular frequency (5 rad s^{-1}) until the gels' elastic modulus, G', plateaued for at least 15 min. The temperature was then raised to 37°C and the gel was allowed to equilibrate for 2 min. A second time sweep was conducted until G' plateaued for at least 15 min. For each new sample an oscillatory stress sweep was then performed (0.1 – 100 Pa oscillatory stress, 5 rad s^{-1} angular frequency) to determine the linear viscoelastic range from which an oscillatory stress was chosen and applied to all subsequent experiments at that condition. Oscillatory frequency sweeps were then performed at a controlled oscillatory stress (ranging from 1.5 to 50 Pa) determined from the linear viscoelastic region of oscillatory stress sweeps (0.001 –0 100 rad s^{-1} angular frequency depending on the gel's crossover frequency characteristics). Dynamic gel strength ($G'_{plateau}$) was calculated as the average G' from the plateau region of each oscillatory frequency sweep. For pH 4.8 where no defined plateau was exhibited, the $G'_{plateau}$ was determined by averaging the G' values above the crossover frequency. The characteristic relaxation time, **τ**, was then calculated as:

$$\tau = 2\pi/\omega_c \quad (1)$$

where ω_c is the crossover frequency in Hertz and is determined from the angular frequency at which G' equals G". All experiments were done in triplicate unless otherwise noted.

Simple Viscosity

The simple viscosity was measured using the same apparatus, geometry, and formulation as above for a pH 4.8 sample. A steady state flow was applied from shear rates of 0.06 to 1.1 s^{-1} at 37°C. These shear rates correspond to the lag times where diffusion occurred on the ensemble-averaged MSD plots that were used to determine viscosity from the Stokes-Einstein equation. Four samples were analyzed. The viscosity was determined by averaging over the entire data range. Results are reported as the mean.

Tracking Fluorescently-Tagged HIV-1

To generate fluorescently labeled HIV, proviral plasmids encoding the R9 strain virus with an BaL envelope were transfected into 293T cells along with a plasmid encoding a Gag protein with a C-terminal Cherry Fusion [45]. The transfected cells were washed after 24 hours and viral supernatant was harvested at 48 hours post transfection. Virus was purified and concentrated by ultracentrifugation through a 30% sucrose cushion. All viral preps used had a p24 concentration between 800 and 1200 ng ml^{-1}. Individual polymer solutions of **1**

and **2** were prepared at 82.5 mg mL^{-1} in 100 mM buffers at the pH of interest with an ionic strength of 100 mM, adjusted with NaCl. Polymer solutions, 20 μL, were diluted with 2 μL of concentrated Gag-cherry labeled HIV-1 (BaL strain) in Dubelco's modified eagles media (DMEM High Glucose, 4.0 mM L-Glutamine, 4500 mg L^{-1} Glucose, and no Sodium Pyruvate (0.1 um sterile filtered) with 10% fetal bovine serum (FBS) and 50 μg mL^{-1} penicillin/streptomycin) and vortexed. Gels were prepared by mixing 15 μL **1**-plus-virus solution with 15 μL **2**-plus-virus solution at the desired pH and vortexing. The gel was removed with either a positive displacement pipette or a small spatula and placed at the center of a silicone sealed 5 mm well on a Delta T4 culture dish (0.17 mm) (Bioptechs Inc.) and topped with mineral oil to prevent evaporation. All imaging was done at 37°C in a temperature controlled chamber. Five image stacks at different locations in the gel were taken using a 100× oil immersion objective (NA 1.4) on a DeltaVision Core microscope system (Applied Precision LLC) with an EMCCD camera using SoftWorx software. Images were collected using an 85 msec time lapse for 60 sec with a 50 msec exposure and a bin of 2. To minimize wall effects images were collected at least 50 μm into the gel. Movies were converted to an 8 bit tiff stack using ImageJ (NIH).

The mean squared displacement (MSD) of virions as a function of gel pH was measured by analyzing their trajectories in the gels at each experimental condition using IDL (ITT Visual Information Solutions) with particle tracking macros. Viral trajectories and the individual and ensemble-averaged MSD were extracted using algorithms developed and kindly provided by John Crocker, David Grier, and Eric Weeks [35]. The individual and ensemble-averaged MSD, were determined across four to five image stacks to increase the number of virions tracked (N ~ 5–10 per image frame) from, $< \Delta r(t)^2 >=< \Delta x^2 + \Delta y^2 >$. After the tracks and individual $<\Delta r^2(t)>$ values were determined, each virion was identified in the movie and its track was visually validated. Imaging was performed in two different pH 4.5 samples to verify results. We calibrated and validated the particle tracking algorithm by tracking 100 nm and 50 nm sulfate modified latex polystyrene particles (Aldrich) in a Newtonian fluid of 99:1 glycerin:water (w w^{-1}) solution. The experimentally determined two dimensional ensemble-averaged MSD can then be used to calculate the diffusion coefficient by fitting a line to the $<\Delta r(t)^2>$ versus t plot to determine the slope and dividing it by four for 2-dimensional space:

$$D_o = \frac{<\Delta r(t)^2>}{4t} \quad (2)$$

And then using the diffusion coefficient in the Stokes-Einstein equation to determine viscosity, η,

$$D_o \frac{k_B T}{6\pi\eta a} \quad (3)$$

where k_B is Bolzmann's constant, T is the absolute temperature, and a is the particle radius.

Nanoparticle tracking

Experiments performed on latex nanoparticles were conducted similarly to the HIV-1 experiments. Individual solutions of **1** and **2** were prepared at 82.5 mg mL^{-1} in 100 mM buffers of the appropriate pH with an ionic strength of 100 mM, adjusted with NaCl. Polymer solutions, 20 μL, were diluted with 2 μL fluorescently labeled beads (0.011% v/v in DMEM – identical to that used for HIV-1 tracking) to give a final polymer concentration of 75 mg mL^{-1} and a bead concentration of 0.001% v/v for the 100 nm and 50 nm red fluorescently labeled sulfate modified polystyrene (Aldrich). Gels were prepared for analysis as above in sealed wells on a Bioptechs Delta T4 culture dish.

Experiments were carried out on a Bioptech microscope stage at 37°C. Particle movement was recorded using a gated intensified camera (Solamere XR/MEGA-10) mounted on an inverted epifluorescence confocal microscope (Olympus 1×70) equipped with a 100× oil immersion objective (Zeiss HAL 100, 1.4 NA) for the 50 nm beads and a 60× oil immersion objective (Zeiss HAL 60, 1.3 NA) for the 100 nm beads. Movies were captured using InVivo Analyzer (MediaCybernetics) in time lapse mode with a burst collection of 2,000 images at a rate of 15 images per second and a bin of 2. To minimize wall effects, samples were collected at least 50 μm into the gel. Images were converted to an 8-bit tiff stack using ImageJ (NIH, Bethesda, MD). Stacks were analyzed using the same protocol as virus.

Determination of Tracking Resolution

The particle-tracking resolution of the setup used in this study was determined by fitting the MSD of the 100 nm and 50 nm sulfate modified polystyrene particles moving in a homogeneous medium (99% glycerol, 1% water (w w^{-1}) to

$$<\Delta r(t)^2>=2\sigma^2+4D_o t \quad (4)$$

where σ is the tracking resolution [35]. For the 100 nm beads σ = 18.5 nm, for the 50 nm beads σ = 24 nm and for HIV-1 σ = 20 nm.

5. References

[1]. Uchegbu, IF.; Schatzlein, AG. in Polymers in Drug Delivery. Taylor & Francis, Inc; 2006. p. 1-22.

[2]. Topp S, Prasad V, Cianci GC, Weeks ER, Gallivan JP. J. Am. Chem. Soc. 2006; 128:13994–13995. [PubMed: 17061859]

[3]. Alvarez-Lorenzo C, Concheiro A. Mini Rev. Med. Chem. 2008; 8:1065–1074. [PubMed: 18855723]

[4]. Traitel T, Goldbart R, Kost J. J. Biomater. Sci. Polym. Ed. 2008; 19:755–767. [PubMed: 18534095]

[5]. Cutler B, Justman J. Lancet Infect. Dis. 2008; 8:685–697. [PubMed: 18992405]

[6]. Okado, HH. in Vaginal Drug Delivery. Taylor and Francis Inc; NY: 2001.

[7]. Tevi-Benissan C, Belec L, Levy M, Schneider-Fauveau V, Si Mohamed A, Hallouin MC, Matta M, Gresenguet G. Clin. Diagn. Lab Immunol. 1997; 4:367–374. [PubMed: 9144379]

[8]. Maher D, Wu X, Schacker T, Horbul J, Southern P. Proc. Natl. Acad. Sci. 2005; 102:11504–11509. [PubMed: 16061810]

[9]. Hladik F, McElrath MJ. Nat. Rev. Immunol. 2008; 8:447–457. [PubMed: 18469831]

[10]. Hladik F, Sakchalathorn P, Ballweber L, Lentz G, Fialkow M, Eschenbach D, McElrath MJ. Immunity. 2007; 26:257–270. [PubMed: 17306567]

[11]. Haase AT. Nat. Rev. Immunol. 2005; 5:783. [PubMed: 16200081]

[12]. Hladik F, Hope TJ. Current HIV/AIDS Reports. 2009; 6:20–28. [PubMed: 19149993]

[13]. Geonnotti AR, Katz DF. Biophys. J. 2006; 91:2121–2130. [PubMed: 16815899]

[14]. Geonnotti, AR, III.. Ph.D Thesis. Duke University; Durham, NC: 2008.

[15]. Owen DH, Peters JJ, Kieweg SL, Geonnotti AR, Schnaare RL, Katz DF. J. Pharm. Sci. 2007; 96:661–669. [PubMed: 17131365]

[16]. Roberts MC, Hanson MC, Massey AP, Karren EA, Kiser PF. Adv. Mater. 2007; 19:2503–2507.

[17]. Roberts MC, Mahalingam A, Hanson MC, Kiser PF. Macromolecules. 2008; 41:8832–8840.

[18]. Wiley JP, Hughes KA, Kaiser RJ, Kesicki EA, Lund KP, Stolowitz ML. Bioconjug. Chem. 2001; 12:240–250. [PubMed: 11312685]

[19]. Stolowitz ML, Ahlem C, Hughes KA, Kaiser RJ, Kesicki EA, Li G, Lund KP, Torkelson SM, Wiley JP. Bioconjug. Chem. 2001; 12:229–239. [PubMed: 11312684]

[20]. Springsteen G, Wang B. Tetrahedron. 2002; 58:5291–5300.

[21]. Vandenburg YR, Zhang Z-Y, Fishkind DJ, Smith BD. Chem. Commun. 2000; 2:149–150.

[22]. Tatjana Levy CDGBS. Adv. Funct. Mater. 2008; 18:1586–1594.

[23]. Loughlin RG, Tunney MM, Donnelly RF, Murphy DJ, Jenkins M, McCarron PA. Euro. J. Pharm. Biopharm. 2008; 69:1135–1146.

[24]. Roberts, MC. Ph.D Thesis. University of Utah; Salt Lake City: 2008.

[25]. Haag R, Kratz F. Angew. Chem. Int. Ed. 2006; 45:1198–1215.

[26]. Sijbesma RP, Beijer FH, Brunsveld L, Folmer BJB, Hirschberg JHKK, Lange RFM, Lowe JKL, Meijer EW. Science. 1997; 278:1601–1604. [PubMed: 9374454]

[27]. Robb ID, Smeulders JBAF. Polymer. 1997; 38:2165–2169.

[28]. Pezron E, Ricard A, Lafuma F, Audebert R. Macromolecules. 1988; 21:1121–1125.

[29]. Schultz RK, Myers RR. Macromolecules. 1969; 2:281–285.

[30]. Kieweg SL, Katz DF. J Biomech Eng. 2006; 128:540–553. [PubMed: 16813445]

[31]. Kieweg SL, Katz DF. J Pharm Sci. 2007; 96:835–850. [PubMed: 17094142]

[32]. Power DJ, Rodd AB, Paterson L, Boger DV. J. Rheol. 1998; 42:1021–1037.

[33]. Gentile M, Adrian T, Scheidler A, Ewald M, Dianzani F, Pauli G, Gelderblom HR. J. Virol. Methods. 1994; 48:43–52. [PubMed: 7962259]

[34]. McDonald D, Vodicka MA, Lucero G, Svitkina TM, Borisy GG, Emerman M, Hope TJ. J. Cell Biol. 2002; 159:441–452. [PubMed: 12417576]

[35]. Crocker JC, Grier DG. J. Colloid Interf. Sci. 1996; 179:298–310.

[36]. Valentine MT, Kaplan PD, Thota D, Crocker JC, Gisler T, Prud'homme RK, Beck M, Weitz DA. Phys. Rev. E. 2001; 64:061506–061515.

[37]. Lai SK, O'Hanlon DE, Harrold S, Man ST, Wang Y-Y, Cone R, Hanes J. Proc. Natl. Acad. Sci. 2007; 104:1482–1487. [PubMed: 17244708]

[38]. Cu Y, Saltzman WM. Mol. Pharmaceutics. 6:173–181.

[39]. Dawson M, Krauland E, Wirtz D, Hanes J. Biotechnology Progr. 2004; 20:851–857.

[40]. Suk JS, Suh J, Lai SK, Hanes J. Exp. Biol. Med. 2007; 232:461–469.

[41]. Valentine MT, Perlman ZE, Gardel ML, Shin JH, Matsudaira P, Mitchison TJ, Weitz DA. Biophys. J. 2004; 86:4004–4014. [PubMed: 15189896]

[42]. Cutalo JM, Deterding LJ, Tomer KB. J. Am.Soc. Mass Spectrom. 2004; 15:1545–1555. [PubMed: 15519221]

[43]. Zhu X, Borchers C, Bienstock RJ, Tomer KB. Biochemistry. 2000; 39:11194–11204. [PubMed: 10985765]

[44]. Grant RM, Hamer D, Hope T, Johnston R, Lange J, Lederman MM, Lieberman J, Miller CJ, Moore JP, Mosier DE, Richman DD, Schooley RT, Springer MS, Veazey RS, Wainberg MA. Science. 2008; 321:532–534. [PubMed: 18653884]

[45]. Leblanc JJ, Perez O, Hope TJ. J. Virol. 2008; 82:2570–2574. [PubMed: 18094163]

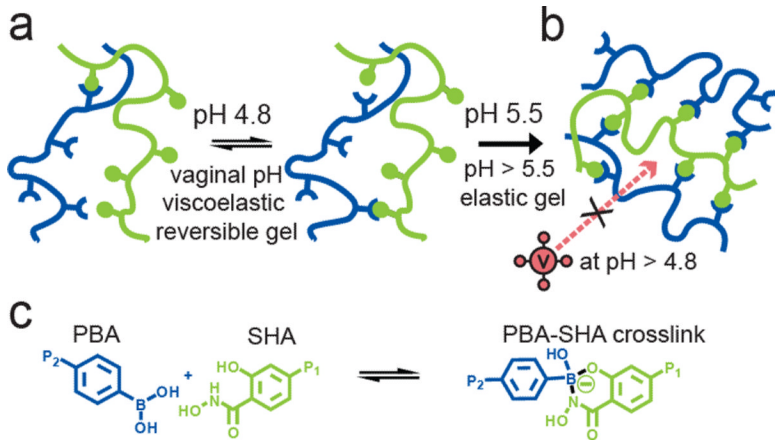

Scheme 1.

The pH sensitive equilibrium between polymer bound PBA and SHA results in reversible covalent crosslinks that provide pH modulation of the viscoelastic behavior of PBA-SHA crosslinked hydrogels. a) Depiction of the pH sensitive equilibrium of polymer bound PBA (blue) and polymer bound SHA (green). At vaginal pH (pH 4.5 to 5) the PBA-SHA crosslink rapidly hydrolyzes and reforms yielding reversible viscoelastic gels. b) Above pH 5.5 the rate of hydrolysis decreases resulting in more permanently covalent crosslinks and elastic gel behavior. c) Chemical scheme of the equilibrium between the unbound PBA and SHA moieties and the PBA-SHA crosslink.

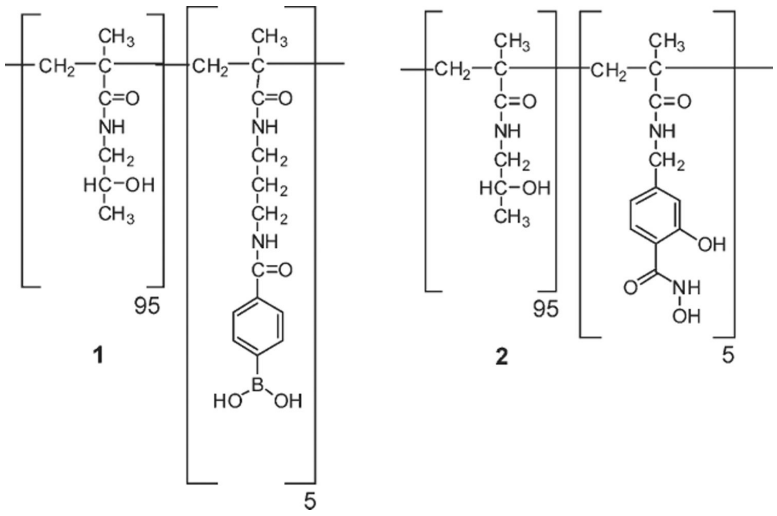

Figure 1.
Chemical structures of p(HPMAm$_{95}$-APMAmPBA$_5$) (**1**) and p(HPMAm$_{95}$-MAAmSHA$_5$) (**2**).

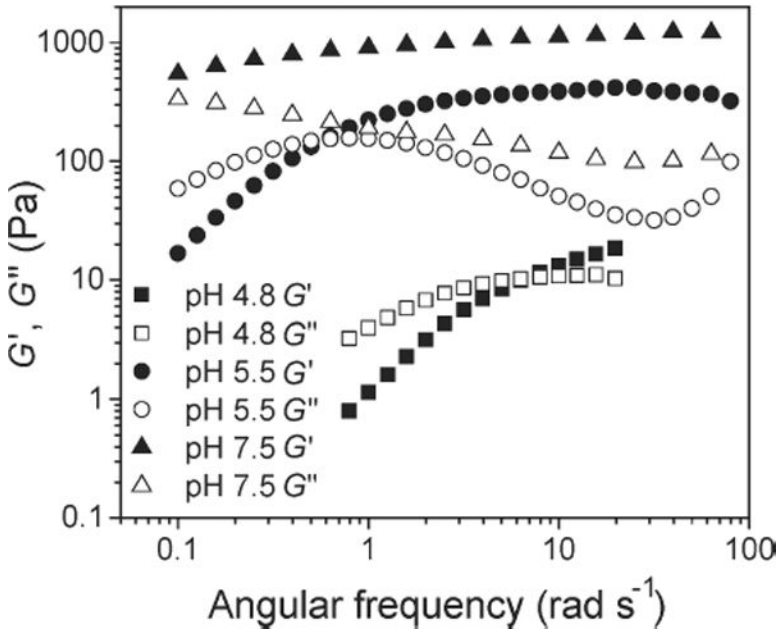

Figure 2.

Frequency dependent viscoelastic behavior of the PBA-SHA crosslinked gel over the pH range experienced in the vaginal lumen. Storage modulus (G') and loss modulus (G") versus angular frequency for the gel at pH 4.8, 5.5 and 7.5 at 37°C. Note the progressive decrease of the frequency at which the crossover between G' sand G" occurs with increasing pH. N=3, mean.

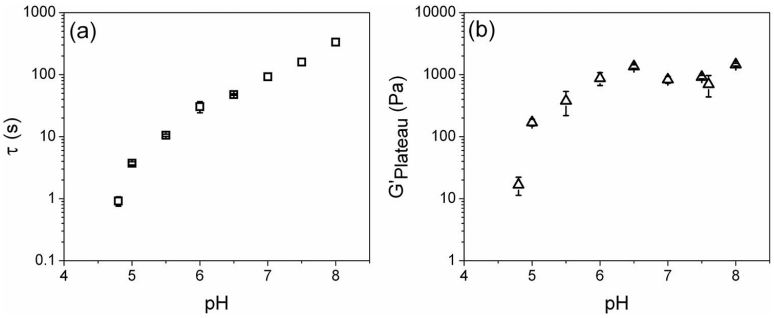

Figure 3.

Effect of pH on viscoleastic properties. a) Characteristic relaxation time (**τ**) and b) $G'_{Plateau}$ over the vaginal pH range of 4 to 8 at 37°C. The characteristic relaxation time steadily increased throughout the pH range, whereas the G'Plateau was only impacted below pH 6. N = 3, mean ± SD, except (a) pH 7, 7.5 and 8.0, N =1.

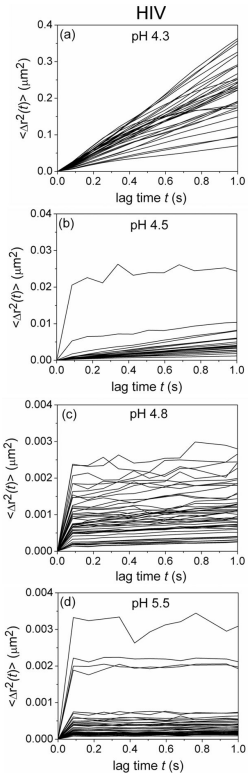

Figure 4.

Transport of Gag-Cherry labeled HIV-1 (BaL strain) in the PBA-SHA crosslinked gel at 37°C as a function of pH. a–d) The mean squared displacement of the individual virions ($<\Delta r^2(t)>$, μm^2) as a function of the lag time (t, s). Five image stacks were taken with between 25–60 virion trajectories tracked total.

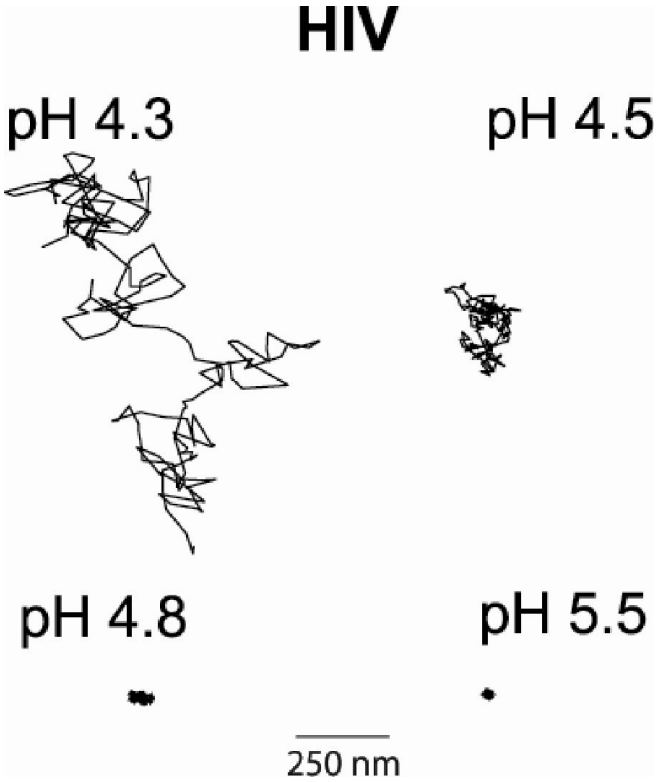

Figure 5.
Representative trajectories of a virion in the gel at each tested pH. The virions at pH 4.3 and pH 4.5 were tracked for 17 s, while the pH 4.8 and pH 5.5 virions were tracked for 60 s. Note that at pH 5.5 we are tracking at the noise level.

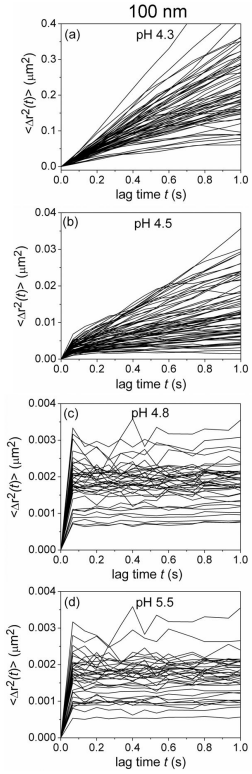

Figure 6.

Transport of 100 nm sulfate modified latex particles in the PBA-SHA crosslinked gel at 37°C as a function of pH. a–d) The mean squared displacement of a random sample of individual 100 nm beads ($<\Delta r^2(t)>$, μm^2) as a function of lag time (t, s). Three to five image stacks in each sample were taken with over 100 particle trajectories tracked total.

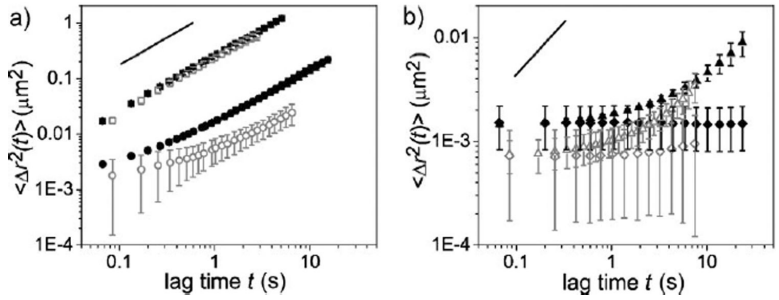

Figure 7.

Ensemble-averaged mean squared displacement for HIV-1 (blue, open symbols) and 100 nm fluorescently labeled sulfate modified latex particles (black, closed symbols) moving in the PBA-SHA crosslinked polymers as a function of pH. a) The ensemble-averaged MSD at pH 4.3 (□) and pH 4.5 (◯). b) The ensemble-averaged MSD at pH 4.8 (Δ) and pH 5.5 (◇). The ensemble-averaged MSD from three to five image stacks imaged from the same sample were averaged, mean ± SD. The solid line depicts a slope of one.

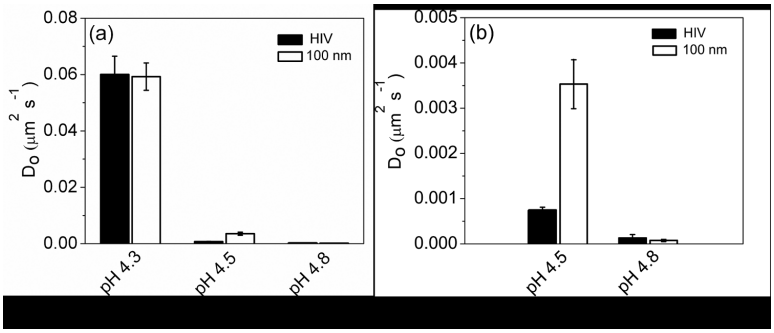

Figure 8.

The diffusion coefficients (D_o) for Gag-cherry labeled HIV (BaL strain) compared to 100 nm fluorescently labeled sulfate modified latex particles. a) Comparison of D_o at pH 4.3, 4.5 and 4.8. The pH 4.8 values are just above the baseline. b) Comparison of D_o at pH 4.5 and pH 4.8. The diffusion coefficient is determined by taking one-fourth of the slope for the ensemble-average MSD versus *t* for each particle.